LI, Hangxin; WANG, Shengwei. Coordinated optimal design of zero/low energy buildings and their energy systems based on multi-stage design optimization. Energy, 2019, 189: 116202.

https://doi.org/10.1016/j.energy.2019.116202



# Coordinated optimal design of zero/low energy buildings and their energy systems based on multi-stage design optimization

Hangxin Li and Shengwei Wang*

Department of Building Services Engineering, The Hong Kong Polytechnic University, Kowloon, Hong Kong

**Abstract:** As promising means to reduce carbon emission and energy consumption, zero/low energy buildings have been attracting increasing attentions. Multi-stage design optimization methods have been developed for zero/low energy buildings and their energy systems especially when a large number of design variables need to be optimized. However, these methods ignore the interactions between building envelope and energy system design optimizations, which can be addressed by simultaneous optimization methods requiring huge computation cost. In this study, a coordinated optimal design method is proposed as a computation cost-effective method for stand-alone and grid-connected zero/low energy buildings and their energy systems on the basis of multi-stage design optimization methods, to effectively consider the interactions between building envelope and energy system design optimizations. An iterative approach is adopted to coordinate multi-stage optimizations of building envelope and energy systems. The Hong Kong zero carbon building is used as the reference building to test and validate the proposed method. The results and experiences of the case studies show that the proposed coordinated design method can provide global optimal designs efficiently and robustly. The life cycle "cost" of the optimal designs is 4% less and unmet cooling load is over 22% less compared with existing multi-stage design methods.

**Keywords:** design optimization; multi-stage design optimization; zero energy building; low energy building; energy system.

*Corresponding author: Shengwei Wang, email: beswwang@polyu.edu.hk

**Nomenclature**

| | |
|---|---|
| $A$ | area ($m^2$) |
| $Cap$ | design capacity (kW) |
| $COP$ | coefficient of performance of chiller |
| $D_{dis}$ | winter thermal discomfort |
| $E$ | energy storage (kWh) |
| $F$ | optimization objective |
| $FC$ | fuel consumption (kW) |
| $GII$ | grid impact index |
| $IC$ | initial cost (USD) |
| $K$ | temperature coefficient of the maximum generation power of PV panels (1/K) |
| $NCC$ | number of charge cycles |
| $OC$ | operation cost (USD) |
| $P$ | power (kW) |
| $Q$ | load (kW) |
| $RC$ | replacement cost (USD) |
| $RPC$ | rotor power coefficient |
| S | coordinating design variables |
| $T$ | temperature (°C) |
| $TC$ | total cost (USD) |
| $X$ | vector of design variables |
| $Y$ | vector of design inputs |
| $a$ | penalty ratio for thermal discomfort |
| $a1$ | penalty ratio for unmet power |
| $a2$ | penalty ratio for unmet cooling load |
| $a3$ | penalty ratio for grid impact index |
| $c$ | unit price |
| $f$ | partial load |
| $g(\cdot)$ | equality design constraints |
| $h(\cdot)$ | inequality design constraints |
| $k$ | years in building life cycle |
| $m$ | flow rate ($m^3/s$) |

$r$ solar radiation (kW/m$^2$)

$t$ time

$v$ velocity (m/s)

$w$ the number of chillers in operation

*Greek letters*

$\eta$ efficiency

$\rho$ air density (kg/m$^3$)

$\Delta t$ time interval

*Subscripts*

*AC* absorption chiller

*AHU* air handling units

*AL* standalone

*CG* co-generators

*CL* cooling load

*CT* cooling tower

*EC* electric chillers

*EL* electricity load

*GC* grid-connected

*PV* photovoltaic

*WT* wind turbines

*air* air

*amb* ambient

*bat* battery

*cell* cell

*ch* battery charge

*clp* cooling water pumps

*cw* chilled water

*cwp* chilled water pumps

*dch* battery discharge

*dem* demand

*design* design value

| | |
|---|---|
| *ele* | electricity |
| *env* | envelope |
| *ex* | export |
| *hr* | heat recovery |
| *hub* | hub of wind turbine |
| *i* | count number |
| *im* | import |
| *inv* | inverter |
| *j* | count number |
| *max* | the maximum value |
| *min* | the minimum value |
| *ref* | reference |
| *sup* | supply |
| *sys* | system |
| *umt* | unmet |

## 1. Introduction

Energy conservation and environmental protection are the critical issues faced by the sustainable development of human societies. To meet the 1.5 K goal of the UNFCCC Paris Agreement [1], many countries have set their objectives for the reduction of carbon dioxide emission and energy consumption. For example, Hong Kong has set its target to reduce carbon emissions to 3.3-3.8 tonnes per capita (equivalent to a reduction of 26%-36%) by 2030 [2]. Buildings play significant roles in achieving these objectives as they account for over 40% of end-use energy worldwide [3] and 80% of end-use energy (up to 90% of electricity) in Hong Kong [4]. Zero/low energy buildings, as efficient means to reduce carbon emission and energy consumption, have been attracting increasing attentions from governments, professionals and society in recent years [5-6].

Previous studies about design optimization of zero/low energy buildings mainly addressed three tasks, including: design optimization of building envelope only [7-8], design optimization of building energy systems only [9-17], and design optimization of both building envelope and energy systems [18-29]. The design optimization methods for both building envelope and energy systems, which is the target of this study, can be classified as two main categories. The first category is "simultaneous design optimization method". The methods in this category aim at optimizing design variables of building envelope and energy system simultaneously [18-22]. Marszal and Heiselberg [18] explored the cost optimal design for a residential net-zero-energy building in Denmark by searching among three levels of building envelope design and three alternatives of energy system design. Georges et al. [19] investigated a single-family dwelling in Belgium by analyzing the combinations of sixteen heating systems and five building designs. Optimal designs were selected among limited number of possible design solutions in these studies [18-19, 23]. More effective optimization tools/algorithms were introduced for effective search among wider search spaces with lower computation cost. Ferrara et al. [20] optimized 10 design variables of building envelope and the associated technical system using Genopt as the optimizer and TRNSYS as the simulation tool. More than $6\times10^3$ simulations were performed in order to find the optimal design solution among $14\times10^9$ possible design solutions. Hamdy et al. [21] optimized 9 design variables of building envelope and energy supply system for a nearly zero energy building using GenOpt. 18,000 - 400,000 evaluations were performed to identify the cost optimal design solution among 1,306,368 possible design solutions using three different optimization algorithms.

It is found that the computation costs of these methods highly depend on the settings of the optimization algorithms and the number of variables to be optimized. For example, the computation cost of GA generally increases exponentially with the increased number of design variables to be optimized. In addition, the use of simulation software tools for evaluating building envelope and energy systems can further increase the computation cost and complexity of design optimization. In fact, as stated by Ting [30], it is extremely difficult to achieve the optimal design using simultaneous optimization methods when the number of design variables is too large.

The second category is "multi-stage design optimization method". Most methods in this category break down the whole design optimization task into several subtasks and effective optimization algorithms/tools are adopted to speed up the search in each of the subtasks [23-29]. For example, Hamdy et al. [23] proposed a multi-stage optimization method. In the first stage, design variables of building envelope and heat recovery unit are optimized to minimize the primary energy consumption of a building. In the second stage, optimal heating/cooling system is identified by assessing the financial and environmental viability of the combinations of heating/cooling systems and the selected building envelope designs. In the third stage, renewable energy system is optimized for the objective of cost minimization while subject to sufficient energy production. After breaking down the optimization task into three subtasks, optimization was achieved by only 3,200 evaluations to optimize 11 design variables which would need to evaluate more than $3\times10^9$ design options if exhaustive search was applied. Kurnitski et al. [24] proposed a seven-step procedure to minimize the life cycle cost of nearly zero energy buildings. Where, 7 design variables were optimized in 2 stages. Rysanek and Choudhary [25] decoupled the whole-building optimization of 17 variables into three stages for expedient exhaustive search of low-carbon and low-energy building refurbishment options. Ascione et al. [27-29] proposed multi-stage design optimization methods for building design and retrofitting respectively. The whole design optimization task was divided into two main stages: envelope design optimization and energy system design optimization. The multi-stage design optimization methods reduce computation cost greatly by avoiding unfeasible combinations of building envelope and energy system designs [23]. However, these existing multi-stage optimization methods assume no impacts of energy system design optimization on the optimal envelope design and ignore the possible interactions between building envelope and building energy systems. The optimal solutions achieved are "local optimal

solutions" of building envelope and energy systems separately rather than "global optimal solutions" considering the building envelope and the energy system as a whole.

This study therefore proposes a coordinated optimal design method for zero/low energy buildings and their energy systems on the basis of the existing multi-stage design optimization methods to consider the interactions between building envelope and energy system design optimizations. The main innovation and benefits are that the proposed method keeps the high efficiency and flexibility of the existing multi-stage design optimization methods and, at the same time, achieves the same effect (i.e., global optimal solution of building envelop and energy systems) of the simultaneous design optimization methods. An iterative optimization approach is adopted to coordinate multi-stage design optimizations of building envelope and energy systems. The energy system design variables which have significant impacts on the building envelope design optimization (namely "coordinating design variables" in this paper) are identified and used to build the coordination of the building envelope and energy system design optimizations. The envelope design and energy system design are optimized iteratively using the updated design of each other until the coordinating design variables converge. Three case studies are performed to test and validate the proposed method using the Hong Kong zero carbon building (ZCB) as the reference building. This paper presents the procedure and method of the proposed coordinated design optimization as well as the results of the validation case studies.

## 2. Procedure and method of coordinated design optimization

### 2.1 Procedure and major steps

Existing multi-stage design optimization methods (namely uncoordinated optimal design method in the rest of this paper) generally optimize building envelope and energy system separately without considering the impacts of energy system design optimization on building envelope design optimization as shown in Fig.1A. At Stage 1, the design variables of building envelope are optimized within their searching ranges by considering the impacts of building envelope design optimization on energy system design optimization, since the impacts of building envelope design on the performance of building and energy systems may be adverse. At Stage 2, building loads, such as the electricity and cooling load profiles associated with the optimal envelope design, are then calculated. Based on the load profiles, design variables of the energy systems are optimized

within their searching ranges. The obtained optimal envelope design and energy system design are eventually taken as the optimal design solution for the building.

The proposed coordinated optimal design method coordinates the design optimizations of building envelope and energy systems to consider the interactions between building envelope and energy system design optimizations in order to achieve the global optimal solution or the same effect of the simultaneous optimization, as shown in Fig.1B. The method involves two steps, i.e., the identification of coordinating design variables and the coordinated design optimization. At the first step, the coordinating design variables ($S$) are identified. They are some of the energy system design variables, which have impacts on building envelope optimization. They are considered in the performance assessment at the stage of building envelope design and optimized at the stage of system design optimization.

At the second step, an iterative approach is adopted to coordinate the multi-stage design optimizations. Each iteration (optimization loop) is, in fact, a multi-stage design optimization consisting of building envelope design optimization and energy system design optimization. At the first stage, an initial set of values ($S_i$) is assumed for the coordinating design variables to be used in the performance assessment for building envelope design optimization in order to make a trade-off between building envelope and energy system design optimizations. Building envelope design optimization is conducted to identify the optimal envelope design, which minimizes the optimization objective of envelope design. At the second stage, hourly cooling load and electricity load (excluding electricity for cooling) profiles of the optimal envelope design are calculated using building simulation software. These profiles are used for building energy system design optimization. The optimal energy system design variables including the optimal coordinating design variables are identified to minimize the optimization objective of energy system design, subject to the satisfaction of the energy demands of the optimal envelope design. If the obtained optimal coordinating design variables given by energy system design optimization ($S_i'$) deviates significantly from the value set in the envelope design optimization ($S_i$), a new trial of building envelope optimization will be performed after setting a new $S_{i+1}$ based on the $S_i$ and $S_i'$ at last optimization loop. The new $S_{i+1}$ can be determined as the $S_i'$ at the last optimization loop or the average of the $S_i$ and $S_i'$ at last optimization loop in order to accelerate the convergence. A new optimization loop starts, and building envelope design optimization and energy system design optimization are conducted again under the updated setting. The optimization loop continues until

the deviation between $S_i$ and $S_i'$ in the same loop is less than a preset threshold, $\varepsilon$. $\varepsilon$ is set as 2% in this study by assuming that 2% deviation has negligible impacts on building and system performance. The finally achieved optimal envelope design and optimal energy system design constitute the optimal design solution for the building.

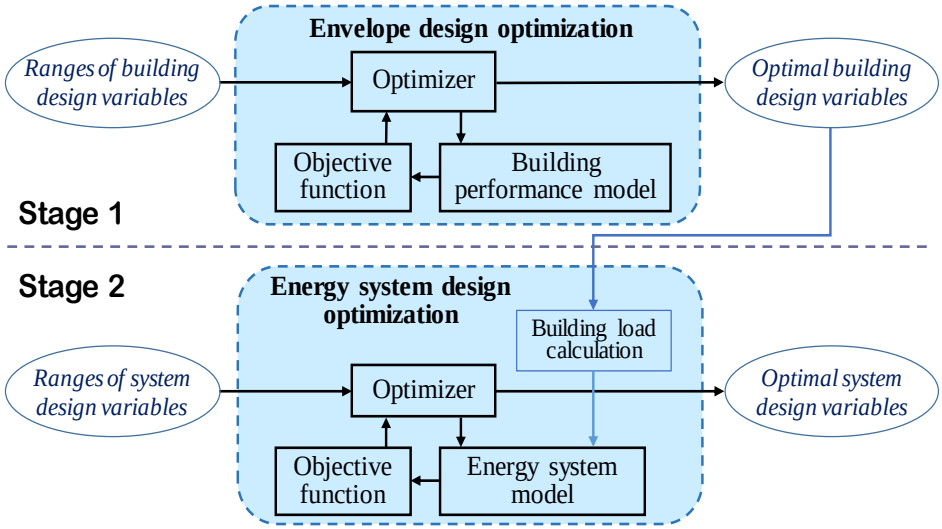


(A) Existing uncoordinated optimal design method

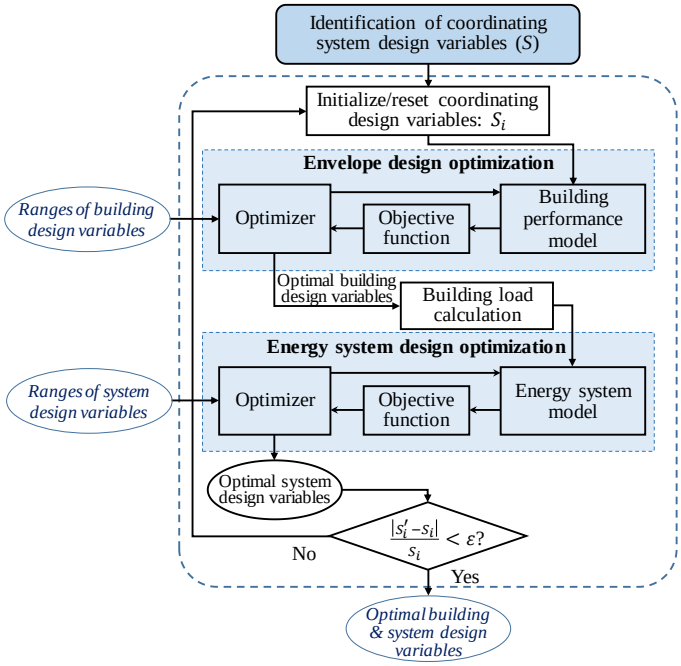


(B) Proposed coordinated optimal design method

**Fig. 1**. Outline of the proposed coordinated optimal design method and the existing uncoordinated optimal design methods

2.2 Formulation of the optimization problems

The design optimization problems of building envelope and energy systems are formulated as Eq. (1) and Eq. (2), respectively. Where, *F* is the design optimization objective. X is the vector of the design variables. Y is the vector of the presumed design inputs. The subscript "*env*" refers to envelope, while subscript "*sys*" refers to energy systems. The design variables of building envelope are optimized within their searching ranges. The design variables of energy systems are optimized within their searching ranges subject to some equality and inequality design constraints.

Envelope design optimization:

$$\text{Minimize: } F_{env}(X_{env}, S_i, Y_{env}) \tag{1}$$

$$\text{subject to: } X_{env,min} \leq X_{env} \leq X_{env,max}$$

System design optimization:

$$\text{Minimize: } F_{sys}(X_{sys}, Y_{sys}) \tag{2}$$

$$\text{subject to: } X_{sys,min} \leq X_{sys} \leq X_{sys,max}$$

$$g(X_{sys}, Y_{sys}) = 0$$

$$h(X_{sys}, Y_{sys}) \leq 0$$

## 3. The validation case, building performance model and energy system models

3.1 Description of the validation case

A simple building is constructed as shown in Fig.2 to investigate the need of coordinated optimal design and validate the proposed coordinated optimal design method. The geometry/layout of this building is revised on the basis of ZCB in Hong Kong [31] by changing windows from the longer side walls to the shorter side walls, which are used in the case studies. The building is considered as one thermal zone only. PV panels are fixed on the slope roof of the building.

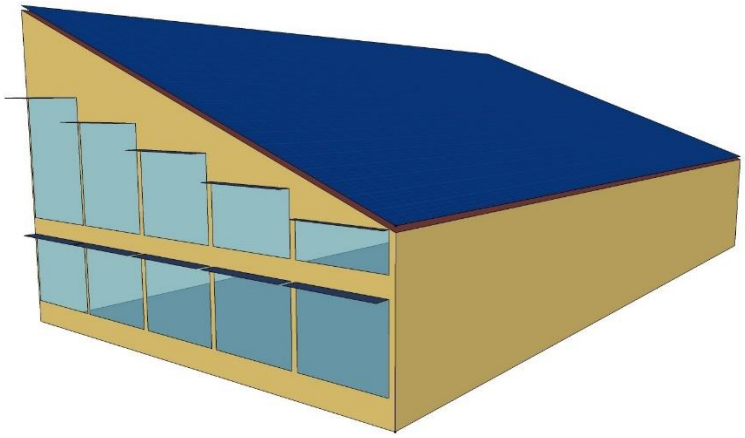

**Fig. 2**. Building architecture model for the validation design case

A typical energy system configuration in subtropical regions is considered for the case studies as shown in Fig. 3. The energy systems mainly consist of three parts: power generation system, air-conditioning system and energy storage system. The power generation system includes PV panels, wind turbines and co-generators. The air-conditioning system mainly consists of absorption chillers, electric chillers, air handling units (AHU), cooling towers, cooling water circulation system and chilled water distribution system. Battery constitutes the energy storage system. Due to the facts that heating is not provided in most subtropical regions, cooling supply is considered only in the case studies, which is provided only in the working hours (8:00-19:00, except Wednesday).

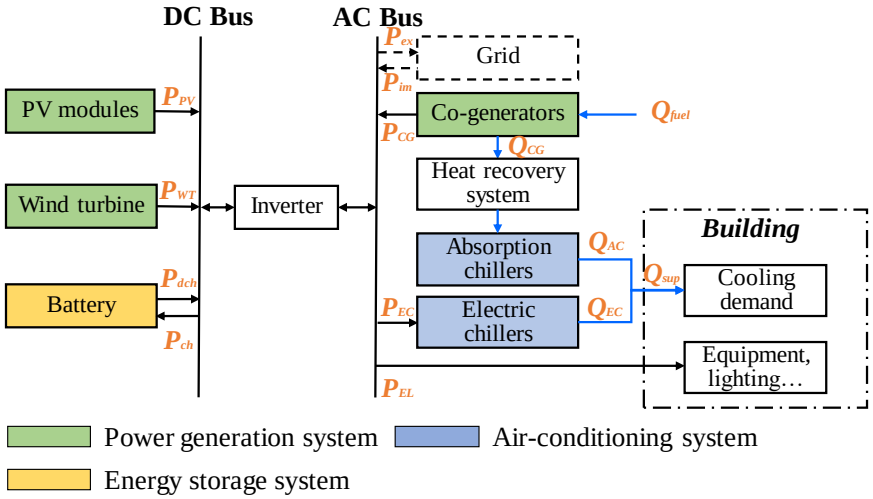


**Fig. 3**. Energy system configuration concerned

3.2 Design variables concerned

Table 1 shows the identified design variables of building envelope and energy systems as well as their searching ranges. Five key envelope design variables are identified for zero/low energy buildings in subtropical regions through a comprehensive sensitivity analysis in a previous study of the authors [7], and optimized in this study. They are building orientation, roof solar absorptance, window-to-wall ratio (WWR), wall solar absorptance, and overhang projection ratio. The U values or thermal inertia of building envelope components, which also have impacts on building performance, are not considered in this study since the results of a few previous studies show that the selected design variables have more significant impacts on building performance than the U values and thermal inertia in subtropical regions [7, 32].

The design optimization of building energy systems in this study focuses on the optimization of component size and number by assuming the type of each system component is selected prior to design optimization. Ten design variables of building energy systems are identified and optimized. They are PV area, number and capacity of wind turbines, number and capacity of co-generators, number and capacity of electric chillers, number and capacity of absorption chillers, and capacity of battery. The minimum values of the capacities of energy system components are determined based on the minimum capacity of available devices in the market, while their maximum values are determined based on the energy demand of the reference building. It is worth noticing that, for a more complex and detailed system optimization, different efficiencies need to be considered for different types of components when the optimal choice of component types is included. Among the design variables, the number of system component is discrete, while the other design variables such as the component capacity and envelope design variables are continuous.

Table 1. Design variables of building envelope and energy systems

| **Category** | **Design variable** | **Abbreviation** | **Searching range** | **Unit** |
|---|---|---|---|---|
| Building envelope | Building orientation | BO | [0,360] | ° |
| | Roof solar absorptance | RSA | [0.1,0.9] | - |
| | Window-to-wall ratio | WWR | [0.2,0.6] | - |
| | Wall solar absorptance | WSA | [0.1,0.9] | - |
| | Overhang projection ratio | OPR | [0.05,0.5] | - |
| | PV area | $A_{PV}$ | [100,1032] | m² |
| | Capacity of wind turbines | $Cap_{WT}$ | [1,40] | kW |

| | | | | |
|---|---|---|---|---|
| Building energy system | Number of wind turbines | $n_{WT}$ | {0,1,2,3} | - |
| | Capacity of co-generators | $Cap_{CG}$ | [30,150] | kW |
| | Number of co-generators | $n_{CG}$ | {1,2,3} | - |
| | Capacity of absorption chillers | $Cap_{AC}$ | [20,200] | kW |
| | Number of absorption chillers | $n_{AC}$ | {1,2,3,4,5} | - |
| | Capacity of electric chillers | $Cap_{EC}$ | [20,200] | kW |
| | Number of electric chillers | $n_{EC}$ | {1,2,3,4,5} | - |
| | Capacity of battery | $Cap_{bat}$ | [10,100] | kWh |

## 3.3 Optimization objectives and design constraints

The design optimizations of low energy buildings and zero energy buildings are both addressed in the case studies, which can be standalone or grid-connected. Different design optimization objectives of energy systems are formulated for standalone and grid-connected buildings. The design optimization objective functions and design constraints for building envelope and energy systems are formulated and illustrated as follows. GA in the global optimization tool box of Matlab is used as the optimization algorithm in this study, which is able to solve the mixed integer optimization problems. A population size of 100 is set for envelope design optimization, while a population size of 200 is set for system design optimization.

### *Optimization objective for building envelope design*

A single objective ($F_{env}$) is formulated as Eq. (3) for building envelope design optimization, which integrates the part to consider energy demands and the part to consider PV power generation ($P_{PV}$). The PV power generation is considered in envelope design optimization since there is conflict in minimizing building energy demand and maximizing PV power generation for the building concerned. The energy demand part consists of the electricity load excluding that for cooling ($P_{EL}$), cooling load ($Q_{CL}$), and energy penalty for winter thermal discomfort ($D_{dis}$). Winter thermal discomfort is considered since there is no heating provision in winter in Hong Kong. It is quantified by normalizing the hourly PMV value [33] below -0.5. The details for the calculation of $D_{dis}$ were introduced in a previous publication of the authors [7]. $a$ is the penalty ratio for thermal discomfort. It is worth noticing that heating load should also be included for the regions where heating is

provided. Summer thermal discomfort also needs to be considered if there is no cooling provision in summer in heating dominated regions.

A typical and constant coefficient of performance (COP) is assumed for cooling supply in the envelope design optimization since the COP of chillers is unknown at the stage of envelope design, which is set as 3 in the case studies. Two weighting factors, $c_{ele}$ and $c_{PV}$, are used to integrate these two parts as a single cost function. $c_{ele}$ is the unit price of buying electricity (USD/kWh). $c_{PV}$ is the unit price of selling electricity generated by PV (USD/kWh). For standalone buildings, $c_{PV}$ is equal to $c_{ele}$. For grid-connected buildings, $c_{PV}$ is the feed in tariff. $\Delta t$ is the time interval, which is set as one hour in this study.

$$F_{env} = \sum_{j=1}^{8760}(c_{ele,j} * \left(P_{EL,j} * \Delta t + \frac{Q_{CL,j}}{COP} * \Delta t + a * D_{dis,j}\right) - c_{PV} * P_{PV,j} * \Delta t) \quad (3)$$

*Optimization objective for building energy systems of standalone zero/low energy buildings*

The optimization objective ($F_{sys,AL}$) for building energy system design of standalone zero/low energy buildings consists of total cost (*TC*), the accumulated unmet power ($\Sigma P_{umt}$) and the accumulated unmet cooling load ($\Sigma Q_{umt}$), in the building life cycle, which is calculated using Eq. (4-5). The total cost *TC* (USD) includes initial cost (*IC*), operation cost (*OC*) and replacement cost (*RC*) in building life-cycle. The total cost over the building life cycle is assessed as the present cost. The initial cost of a system component is calculated by multiplying the unit price of the component by its design capacity and number. An interest rate is considered, as listed in Table 2, to discount the operation cost and replacement cost in the future. The accumulated unmet power is the sum of the hourly unmet power $P_{umt}$ (kW) over the building life cycle, which is induced when power supply is less than power demand. Similarly, the accumulated unmet cooling load is the sum of the hourly unmet cooling load $Q_{umt}$ (kW) over the building life cycle, which is induced when total capacity of chillers is less than the building cooling demand. Two penalty ratios, *a1* and *a2*, are assigned to unmet power and unmet cooling load respectively. *k* refers to the total years in the building life cycle.

$$F_{sys,AL} = TC + \sum_{i=1}^{k}\sum_{j=1}^{8760} a1 * P_{umt,i,j} + \sum_{i=1}^{k}\sum_{j=1}^{8760} a2 * Q_{umt,i,j} \quad (4)$$

$$TC = IC + OC + RC \quad (5)$$

*Optimization objective for building energy systems of grid-connected zero/low energy buildings*

The optimization objective ($F_{sys,GC}$) for building energy system designs of grid-connected zero/low energy buildings consists of total cost ($TC$), the accumulated unmet cooling load ($\Sigma Q_{umt}$), and the accumulated grid impact index ($\Sigma GII$), in the building life cycle, which is calculated using Eq. (6-7). Gird impact index is considered to reduce the stress that the building imposes on the grid because of frequent power import and export. It is the standard deviation of the ratio of the net imported energy to the average energy demand over a month, as shown in Eq. (7). Two penalty ratios, *a2* and *a3*, are assigned to unmet cooling load and grid impact index respectively. *a2* is the same as that in Eq. (4).

$$F_{sys,GC} = TC + \sum_{i=1}^{k}\sum_{j=1}^{8760} a2 * Q_{umt,i,j} + \sum_{i=1}^{k}\sum_{j=1}^{12} a3 * GII_{i,j} \quad (6)$$

$$\mathrm{GII} = \mathrm{std}\left(\frac{P_{im,i}-P_{ex,i}}{\int_{t1}^{t2} P_{dem}dt}\right) \quad (7)$$

*Design constraints for building energy systems*

The constraints for the design optimization of building energy systems include the limit for battery charge and discharge rate, and the limit for battery storage, as shown in Eq. (8-10).

$$0 \le \mathrm{P_{ch}} \le \mathrm{P_{ch,max}} \quad (8)$$

$$0 \le \mathrm{P_{dch}} \le \mathrm{P_{dch,max}} \quad (9)$$

$$E_{bat,min} \le E_{bat} \le E_{bat,max} \quad (10)$$

3.4 Building performance model

A building performance model adopting an artificial neural network (ANN) is used for building performance evaluation in building envelope design optimization in order to reduce the computation time. Though the preparation of the training data is a little time-consuming, it is beneficial as each optimization will involve many trials to test different settings in order to make sure that the global optimal solution is achieved. The design variables of building envelope listed in Table 1 are chosen as the inputs of the ANN building performance model, as well as the coordinating design variables. The outputs of the ANN model are the annual cooling load, annual electricity load (excluding that for cooling) and annual winter thermal discomfort. The input data for training/validation are generated by sampling in the searching ranges of envelope design variables and PV area using Latin hypercube sampling (LHS) method [39]. The output data is

obtained by building simulation under the typical meteorological year (TMY) weather data in Hong Kong using EnergyPlus. The detailed settings for the internal loads (i.e., occupancy, equipment and lighting) and the settings in EnergyPlus refer to a previous study of the authors [7].

### 3.5 Mathematical models of energy system components

*Power generation system*

*PV model*: The power supplied by PV panels is calculated using Eq. (11-12) [14]. Where, $P_{PV}$ is the power (kW) generated by PV panels. $r$ is the solar radiation (kW/m$^2$). $A_{PV}$ is the total area of PV panels (m$^2$). $\eta_{PV}$ is the overall efficiency of PV panels. $K$ is temperature coefficient (1/K) of the maximum generation power of PV panels. In this study, $K$ is set as -3.7×10$^{-3}$. $T_{cell}$ is cell temperature (°C) of PV panels. $T_{ref}$ is cell temperature (°C) at reference condition, which is set as 25°C in this study. $T_{amb}$ is the ambient temperature (°C).

$$P_{PV} = r \times A_{PV} \times \eta_{PV} \times (1 + K(T_{cell} - T_{ref})) \quad (11)$$

$$T_{cell} = T_{amb} + 0.0256 \times r \quad (12)$$

*Wind turbine model*: The power generated by a wind turbine is calculated by Eq. (13-14) [34]. Where, $P_{WT}$ is the power produced (kW) by a wind turbine. $\rho$ is air density (kg/m$^3$). $v_{hub}$ is wind speed (m/s) at the hub elevation of the wind turbine. $A_{WT}$ is rotor area (m$^2$). $RPC$ is rotor power coefficient. $\eta_{WT}$ is the overall efficiency of the wind turbine. This model is valid when $3 \leq v_{hub} \leq 25$ m/s, and the power generated by the wind turbine is 0 when $v_{hub}$ is out of this range.

$$P_{WT} = 0.5 \times \rho \times v_{hub}^3 \times A_{WT} \times RPC \times \eta_{WT} \quad (13)$$

$$RPC = (-2.025 \times 10^{-7} \times v_{hub}^6 + 1.926 \times 10^{-5} \times v_{hub}^5 - 7.421 \times 10^{-4} \times v_{hub}^4 + 1.483 \times 10^{-2} \times v_{hub}^3 - 0.162 \times v_{hub}^2 + 0.887 \times v_{hub} - 1.508) \times 10^{-3} \quad (14)$$

*Co-generator model*: The electricity and heat produced by a co-generator are calculated using Eq. (15) and Eq. (16) [35], respectively. Where, $P_{CG}$ is the electricity (kW) produced by a co-generator. $FC_{CG}$ is fuel consumption (kW). $Q_{CG}$ is the heat (kW) generated by the co-generator. $\eta_{CG}$ is the co-generator efficiency. The efficiency varies with partial electric load of the co-generator ($f_{CG}$), which is calculated by Eq. (17-18) [35].

$$P_{CG} = FC_{CG} \times \eta_{CG} \quad (15)$$

$$Q_{CG} = FC_{CG} \times (1 - \eta_{CG}) \quad (16)$$

$$\eta_{CG} = -0.2 \times f_{CG}^2 + 0.4 \times f_{CG} + 0.1 \quad (17)$$

$$f_{CG} = \frac{P_{CG}}{P_{CG,design}} \quad (18)$$

*Air-conditioning system*

*Electric chiller model*: The electricity required by electric chillers ($P_{EC}$) is calculated using Eq. (19). The COP of chillers ($COP_{EC}$) is assumed as a variable of partial load of chillers ($f_{EC}$), as Eq. (20-21) [36]. Where, *w* is the number of electric chillers in operation.

$$P_{EC} = \frac{Q_{EC}}{COP_{EC}} \quad (19)$$

$$COP_{EC} = -6.563 \times f_{EC}^2 + 10.714 \times f_{EC} + 1.0794 \quad (20)$$

$$f_{EC} = \frac{Q_{EC}}{w \times Cap_{EC}} \quad (21)$$

*Absorption chiller model*: The cooling supplied by absorption chillers ($Q_{AC}$) depends on the heat generated by the co-generators ($Q_{CG}$), heat recovery efficiency ($\eta_{CG}$) of the heat recovery unit and the COP of absorption chillers ($COP_{AC}$). It is calculated using Eq. (22-23) [35]. A constant COP is used for absorption chillers in this study, which is set as 0.7.

$$Q_{AC} = Q_{hr} \times COP_{AC} \quad (22)$$

$$Q_{hr} = Q_{CG} \times \eta_{hr} \quad (23)$$

*Other air-conditioning system models*: The energy models of chilled water pumps (*cwp*), cooling water pumps (*clp*), AHUs and cooling towers (*CT*) are revised on the basis of the models fitted using the operation data of the corresponding energy devices in the ZCB, as shown in Eq. (24-27) [9]. Where, *P* is the power electricity (kW). *m* is flow rate ($m^3/s$). The subscript *cw* represents the chilled water, while the subscript *air* represents air. $Q_{CT}$ is the cooling load of cooling tower (kW).

$$P_{cwp} = 10 \times \frac{m_{cw}}{m_{cw,design}} - 1 \times \left(\frac{m_{cw}}{m_{cw,design}}\right)^2 \quad (24)$$

$$P_{clp} = constant \quad (25)$$

$$P_{AHU} = 8 \times \frac{m_{air}}{m_{air,design}} + 12 \times \left(\frac{m_{air}}{m_{air,design}}\right)^3 \quad (26)$$

$$P_{CT} = P_{CT,design} \times \left(\frac{Q_{CT}}{Q_{CT,design}}\right)^{1.5} \quad (27)$$

*Energy storage system*:

*Battery model*: The energy storage in the battery ($E_{bat}$) is limited within a range in order to prolong the lifetime of battery, as shown in Eq. (10). Its minimum limit is set to be 20% of the battery capacity in this study, while its maximum limit is set to be 80% of the battery capacity. In addition, battery has its maximum limit for charging and discharging power, as shown in Eq. (8-9). The maximum hourly power charging rate is set as 20% of the battery capacity, while the maximum hourly power discharging rate is 50% of the battery capacity. Charge efficiency ($\eta_{ch}$) and discharge efficiency ($\eta_{dch}$) are considered when the battery charges and discharges, respectively, as shown in Fig. 4.

*Modelling of equipment lifetime and degradation:*

Components of energy system have their own lifetime and performance degradation because of aging. The replacement cost is calculated, when a component reaches its lifetime, based on its initial cost considering an interest rate. The lifetime of battery is determined by its calendar life and the number of charge cycles (NCC). Calendar life is the lifetime of battery even when it has never been put into operation, which is assumed to be 10 years in this study. NCC has a maximum limit, as frequent charging and discharging can significantly reduce the lifetime of battery. It is calculated by Eq. (28) [37]. Once NCC or calendar life reaches its maximum limit in the building life cycle, battery is replaced. Besides lifetime, degradation is considered in this study for PV panels. The overall efficiency of PV panels is assumed to degrade by 0.8% [38] each year in their lifetime.

$$NCC(t) = NCC(t-1) + 0.5 \times \left|\frac{E_{bat}(t) - E_{bat}(t-1)}{E_{bat,max} - E_{bat,min}}\right| \quad (28)$$

3.4 Energy system control strategies

The following typical control strategies are implemented in an ideal control model for the performance assessment of system design optimization. The priority (high to low) of power supply is: PV & wind turbines, battery, co-generators and grid. Absorption chillers have higher priority to supply cooling than electric chillers when co-generators are put into operation. At this situation, electric chillers are put into operation when cooling demand cannot be satisfied using absorption chillers only. Only electric chillers are used when co-generators are not in operation. The detailed control strategies of the entire energy system for grid-connected buildings are illustrated in Fig. 4,

including an overall control mode selection (Fig. 4A) and three alternative operation modes (Fig. 4B-D). Where, $P_{sup}$ and $P_{dem}$ are calculated using Eq. (29) and Eq. (30), respectively.

$$P_{sup} = (P_{PV} + P_{WT} + P_{dch}) \times \eta_{inv} + P_{CG} \quad (29)$$

$$P_{dem} = P_{EC} + P_{EL} + P_{ch} \quad (30)$$

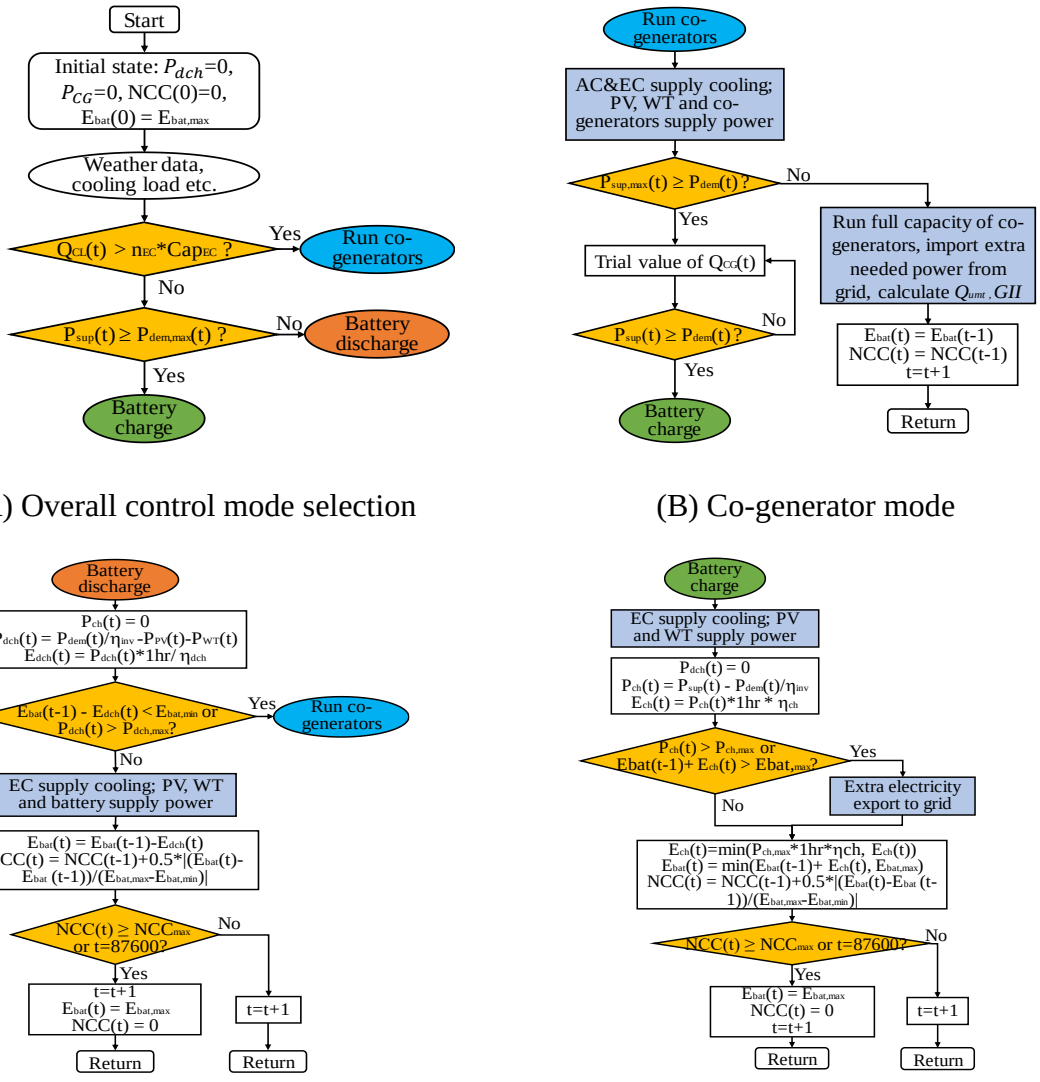


(A) Overall control mode selection

(B) Co-generator mode

(C) Battery discharge mode

(D) Battery charge mode

**Fig. 4**. Control strategies of energy systems at a sampling step for grid-connected buildings

## 4. Identification of coordinating design variables and preprocessing of design optimization

### 4.1 The needs of coordinated design and identification of coordinating design variables

This section elaborates why the interactions between the envelope design and energy system design optimizations (especially the impacts of energy system design optimization on the envelope

design optimization) should be considered, and the identification of the coordinating design variables. Fig.5 shows the variation of building cooling load and PV power generation of the building configuration concerned under different building orientations. The building orientation corresponding to the maximum PV power generation is 15° (from north to east), while the building orientation corresponding to the minimum building cooling load is 270°. It can be seen that the envelope design optimization if considering the minimization of energy demand only would lead to low efficiency of PV power generation and thus lead to higher cost of energy systems. Therefore, there is a need to consider the impacts of the building envelope design on the power generation of PV when optimizing the building envelope design. In fact, it has been considered in the existing multi-stage design optimization of building envelope and energy systems.

Similarly, the design optimization of building energy systems also affects the design optimization of building envelope. For instance, for the building configuration concerned in the validation case, a northern building orientation (i.e., around 0°) may be preferred if the PV area is large, since the benefit of increasing PV power generation efficiency could be higher than the cost of increasing building energy demand. In contrary, an eastern or western building orientation (i.e., around 90° or 270°) may be preferred if the PV area is small, since the loss of decreasing PV power generation efficiency could be lower than the benefit of decreasing building energy demand. Therefore, there is also a need to consider the impacts of energy system design optimization (where the PV design is optimized) on the envelope design when optimizing the building envelope design. However, it is not considered in the existing multi-stage design optimization of building envelope and energy systems.

Coordinated optimal design is therefore needed for buildings. Other examples might be buildings with façade-integrated PV or/and solar windows. For the cases of buildings without system design variables which have significant impacts on building envelope design optimization, coordinated optimal design is not essential as the existing multi-stage optimization methods would provide the same optimization outputs in these cases. Based on the above analysis, the system design variable $A_{PV}$ (i.e., PV area) is eventually selected as the only coordinating design variable in this study.

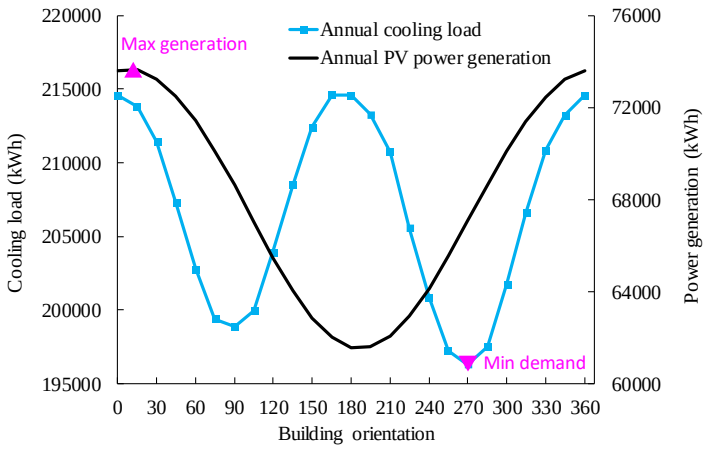


**Fig. 5**. Impacts of building orientation on building cooling load and PV power generation

4.2 Training and validation of ANN model

In this study, the ANN model structure and model parameters (weights) are both optimized in the training process. The mean squared error (MSE) is used to evaluate the performance of ANN model. Firstly, 12,000 sets of training data and 120 sets of validation test data are prepared. Secondly, the optimal ANN model structure is identified using 10-fold cross-validation [40]. Different numbers of hidden layers (1 or 2 hidden layers) and different numbers of neurons in different hidden layers (1-72 neurons when using 1 hidden layer, 1-6 neurons for each layer when using 2 hidden layers) are tested. The results show that the optimal ANN model structure, which has the minimum average MSE in the cross-validation, is one hidden layer with 72 neurons. Its average MSE is $7.95\times10^{-5}$.

At last, the optimal ANN model is obtained by further optimizing the parameters (weights) of ANN model with the optimal model structure. It can be seen from Fig. 6 that the optimal ANN model outputs well match the corresponding target outputs of the test data given by EnergyPlus. Their coefficients of linear regression are all up to 0.999. The consistencies between the impacts of different design variables on the building performance outputs estimated by the ANN model and EnergyPlus are also validated. As an example, Fig. 7 shows the comparisons between the building performance outputs given by ANN model and EnergyPlus when the building orientation varies. It can be seen that the annual electricity loads, cooling loads and winter thermal discomfort given by ANN model and EnergyPlus match very well respectively. In summary, the optimized ANN model has very good accuracy in estimating the building performance including the impacts of individual design variable.

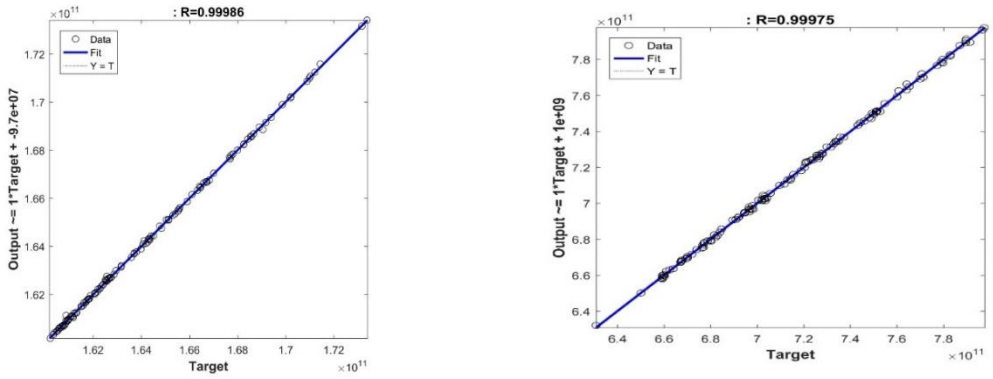


(A) Annual electricity load excluding that for cooling (B) Annual cooling load

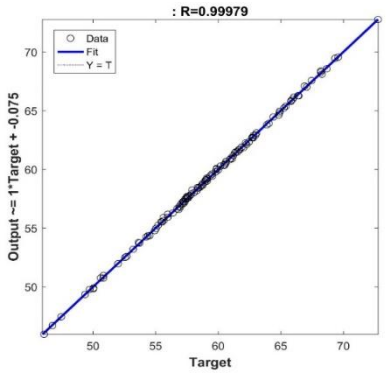


(C) Annual winter thermal discomfort

**Fig. 6**. Outputs of optimal ANN model *vs* target outputs during model validation using test data

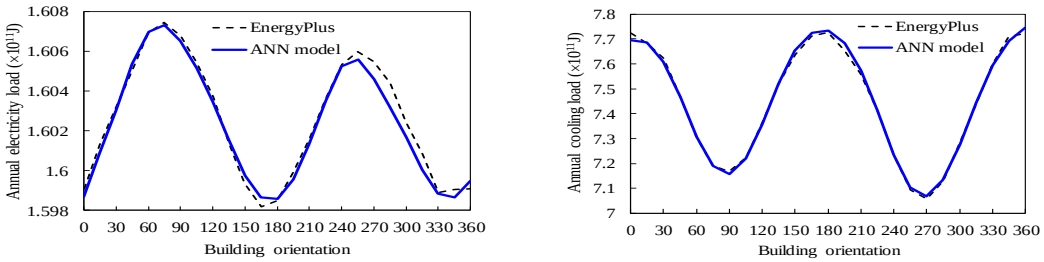


(A) Annual electricity load excluding that for cooling (B) Annual cooling load

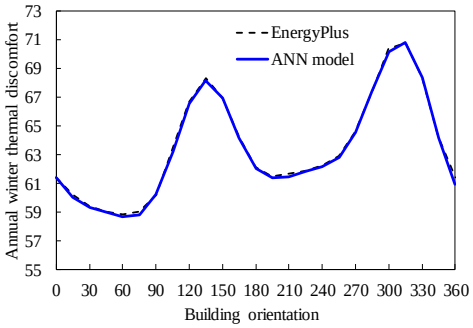


(C) Annual winter thermal discomfort

**Fig. 7**. Outputs of optimal ANN model and EnergyPlus *vs* building orientation

4.3 Selection of penalty ratios for optimization objectives

The penalty ratio *a*, assigned to winter thermal discomfort in the design optimization objective of building envelope, is set as 100 according to a previous publication of the authors [7]. Different *a1* and *a2* are tested in order to identify proper penalty ratios for the design optimization objective of standalone zero/low energy building energy systems (the design optimization of low energy building energy systems are taken as an example). A penalty ratio, which can maintain the corresponding performance indicator within an acceptable level, is considered as a proper penalty ratio. For instance, a proper *a1* is set to make the accumulated unmet power less than a preset level (for example, 1,000 kWh accumulated throughout the building life cycle of 30 years). *a1* is set as different integral multiples of the unit electricity price in Hong Kong (i.e., about 0.15 USD/kWh), while *a2* is assumed to be one third of *a1* in this study by considering an overall COP of 3 for cooling supply. The basic data of energy system models are set according to Table 2 which refers to Ref. [9-11, 14, 34, 35, 41] and 30 years of building life cycle is considered. The optimal system design and its corresponding system performance achieved under different penalty ratios are shown in Table 3. It can be seen that the total cost of the optimal energy system increases with the increase of penalty ratios, while its unmet cooling load decreases. The unmet power of the optimal energy system associated with the penalty ratio *a1* of 0.15 is larger than that associated with the penalty ratio *a1* of 0 (i.e., without considering penalties for unmet power and unmet cooling load). But the unmet power decreases when the penalty ratios further increase. A proper penalty ratio of 9 is finally assigned to the unmet power (i.e., *a1*=9), and a penalty ratio of 3 is assigned to the unmet cooling load (i.e., *a2*=3), since the total cost (*TC*), the accumulated unmet power ($\Sigma P_{umt}$) and the accumulated unmet cooling load ($\Sigma Q_{umt}$) of the corresponding optimal energy system design are within acceptable levels. For the grid-connected zero/low energy buildings, the penalty ratio for grid impact index is determined by assuming that one unit of grid impact index has a cost penalty equivalent to 30% of the total electricity cost in a typical month in this study, i.e., *a3*=240.

Table 2. Basic data of energy system models

| Parameter | Value | Unit |
|---|---|---|
| Unit price of PV | 229.72 | USD/m² |
| Unit price of wind turbine | 2000 | USD/kW |
| Unit price of co-generator | 2400 | USD/kW |

| | | |
|---|---|---|
| Unit price of battery | 213 | USD/kWh |
| Unit price of diesel oil (fuel) | 1.3 | USD/L |
| Unit price of electricity | 0.1472 | USD/kWh |
| Feed in tariff | 0.065 | USD/kWh |
| Interest rate | 8 | % |
| Lifetime of PV | 20 | year |
| Lifetime of wind turbines | 20 | year |
| Lifetime of co-generators | 24000 | hour |
| Lifetime of battery | 10 | year |
| Lifetime of electric chillers | 15 | year |
| Lifetime of absorption chillers | 15 | year |
| Overall efficiency of PV | 0.12 | - |
| Efficiency of wind turbines | 0.9 | - |
| Efficiency of heat recovery system | 0.8 | - |
| Charge efficiency of battery | 0.85 | - |
| Discharge efficiency of battery | 0.85 | - |
| Efficiency of inverter | 0.92 | - |
| Heat value of diesel oil | 39 | MJ/L |

Table 3. Optimal energy system designs and their corresponding performance of the standalone low energy building under different penalty ratios

| Nos. | a1 | a2 | Optimal energy system design | | | | | | | | | | Energy system performance | | |
|---|---|---|---|---|---|---|---|---|---|---|---|---|---|---|---|
| | | | $A'_{PV}$ | $Cap_{WT}$ | $n_{WT}$ | $Cap_{CG}$ | $n_{CG}$ | $Cap_{AC}$ | $n_{AC}$ | $Cap_{EC}$ | $n_{EC}$ | $Cap_{bat}$ | TC | $\Sigma P_{umt}$ | $\Sigma Q_{umt}$ |
| 1 | 0 | 0 | 342.2 | 36.6 | 0 | 30.0 | 1 | 20.0 | 1 | 20.0 | 1 | 99.4 | 549,049 | 17,514 | 2,389,859 |
| 2 | 0.15 | 0.05 | 346.9 | 7.0 | 0 | 30.0 | 1 | 39.2 | 1 | 48.0 | 1 | 98.5 | 594,689 | 61,602 | 394,879 |
| 3 | 2.25 | 0.75 | 460.7 | 19.9 | 0 | 40.0 | 1 | 52.2 | 1 | 73.4 | 1 | 87.4 | 677,154 | 5,986 | 5,297 |
| 4 | 4.5 | 1.5 | 436.1 | 12.7 | 1 | 41.0 | 1 | 53.6 | 1 | 75.1 | 1 | 80.5 | 690,348 | 2,104 | 2,664 |
| 5 | 9 | 3 | 437.5 | 12.7 | 1 | 42.0 | 1 | 54.9 | 1 | 76.5 | 1 | 80.5 | 698,599 | 921 | 1,332 |
| 6 | 18 | 6 | 461.9 | 15.1 | 1 | 44.0 | 1 | 57.5 | 1 | 77.8 | 1 | 84.7 | 708,100 | 221 | 359 |

*Note: The units of variables and objectives refer to that in Table 1 and Eq. (4) respectively.*

## 5. Results of optimization case studies and building performance analysis

### 5.1 Case 1 - Optimal design of a standalone low energy building

Coordinated optimal design is conducted for the validation building with the design intention of standalone low energy building. Two initial PV area settings (1,032 $m^2$ and 100 $m^2$) for envelope design optimization are tested in this case study to verify the effectiveness and robustness of coordinated optimal design method. Table 4 shows the "optimal" design solutions of all optimization loops in these two coordinated design tests. When the initial PV area for envelope design optimization is set as 1,032 $m^2$ (i.e., the maximum PV area), three optimization loops are

needed to reach the convergence as shown in Table 4A. When a PV area of 1,032 $m^2$ is assumed for the envelope design optimization, the cost-optimal PV area given by the system design optimization in order to satisfy the energy demand of the optimized envelope design is 438 $m^2$ only, which deviates significantly from the PV area assumed in envelope design optimization. Therefore, the envelope design achieved is not optimal under the smaller PV area actually given by the system design optimization. A new optimization loop is needed. In this new loop, the PV area is set as 438 $m^2$ in envelope design optimization, which is the optimized PV area given by the system design in the first optimization loop. Under a smaller PV area, the optimal building orientation and overhang projection ratio increase noticeably, leading to the decrease of the PV power generation efficiency and the energy demand. The optimal PV area given by the system design optimization for the new optimized envelope is 461 $m^2$, which still deviates from the PV area setting used in the latest envelope design optimization for over 2%. The third optimization loop is then activated. In this loop, the PV area is set as 449 $m^2$ in envelope design optimization to accelerate the convergence, which is the average of the PV areas used in envelope design optimization and optimized by the system design optimization in the second optimization loop. The optimal PV area given by system design optimization for the new optimized envelope in the third loop is 444 $m^2$, which has a deviation of 1.11%, i.e., within the convergence tolerance of 2%, thus the design optimization converges. The final optimal outputs of the coordinated design optimization under an initial PV area of 1,032 $m^2$ are the outputs of Loop 3 as listed in Table-4A.

When the initial PV area for envelope design optimization is set as 100 $m^2$, four optimization loops are needed to achieve the convergence. The optimal values of both envelope design variables and energy system design valuables are listed in Table 4B. Where, the outputs of Loop 4 are the final optimal outputs of the coordinated design optimization. It can be seen that the optimal design values achieved under the initial PV area setting of 100 $m^2$ are very close to that achieved under the initial PV area setting of 1,032 $m^2$. This indicates that the proposed coordinated optimal design is robust in providing consistent optimal design solutions regardless of the initial settings though different iteration times are needed. In addition, it is practical to achieve the optimal design solution using the coordinated optimal design method. The computation cost is not increased too much (i.e., 3 or 4 times only) compared with the uncoordinated design method (i.e., existing multi-stage design optimization methods).

In contrary, the optimal design solutions achieved by uncoordinated design method under different initial PV area settings are very different, same as the outputs listed in the first row in Table 4A and 4B. The optimal building orientation obtained under a small initial PV area setting is close to east, while the optimal overhang projection ratio is much smaller (about half). The component capacities of the obtained optimal energy system design are obviously larger. This indicates that the uncoordinated design method is not robust in obtaining consistent optimal design solutions under different initial settings. Fig. 8 presents a comparison between the energy performance of the optimal system design solutions obtained using coordinated design method and uncoordinated design method respectively under an initial PV area setting of 100 $m^2$. It can be seen that the optimal design given by coordinated design method provides 4.1% (30,190 USD) less total cost, 22.0% (286 kWh) less accumulated unmet cooling load ($\Sigma Q_{umt}$) and 3.3% (24,044 USD) less energy system design objective value ($F_{sys,AL}$) than that given by uncoordinated design method, although its accumulated unmet power ($\Sigma P_{umt}$) is much higher (by 778 kWh). This indicates that coordinated design method can provide global optimal design solutions, while the optimal design solution achieved by uncoordinated design method is "local" optimum.

Table 4. Optimization loops of coordinated optimal design and optimal design solutions of coordinated and uncoordinated design methods - standalone low energy building

(A) Initial PV area for building envelope design optimization: 1,032 $m^2$

| Loop no. | $A_{PV}$ | Optimal envelope design | | | | | Optimal energy system design | | | | | | | | | |
|---|---|---|---|---|---|---|---|---|---|---|---|---|---|---|---|---|
| | | BO | RSA | WWR | WSA | OPR | $A'_{PV}$ | $Cap_{WT}$ | $n_{WT}$ | $Cap_{CG}$ | $n_{CG}$ | $Cap_{AC}$ | $n_{AC}$ | $Cap_{EC}$ | $n_{EC}$ | $Cap_{bat}$ |
| 1* | 1032 | 7.75 | 0.10 | 0.20 | 0.10 | 0.44 | 438 | 12.7 | 1 | 42.0 | 1 | 54.9 | 1 | 76.5 | 1 | 80.5 |
| 2 | 438 | 8.15 | 0.10 | 0.20 | 0.10 | 0.45 | 461 | 14.0 | 1 | 44.0 | 1 | 57.5 | 1 | 76.6 | 1 | 99.9 |
| **3 (final)** | ***449*** | ***8.05*** | ***0.10*** | ***0.20*** | ***0.10*** | ***0.45*** | ***444*** | ***12.4*** | ***1*** | ***42.0*** | ***1*** | ***54.9*** | ***1*** | ***77.6*** | ***1*** | ***80.9*** |

(B) Initial PV area for building envelope design optimization: 100 $m^2$

| Loop no. | $A_{PV}$ | Optimal envelope design | | | | | Optimal energy system design | | | | | | | | | |
|---|---|---|---|---|---|---|---|---|---|---|---|---|---|---|---|---|
| | | BO | RSA | WWR | WSA | OPR | $A'_{PV}$ | $Cap_{WT}$ | $n_{WT}$ | $Cap_{CG}$ | $n_{CG}$ | $Cap_{AC}$ | $n_{AC}$ | $Cap_{EC}$ | $n_{EC}$ | $Cap_{bat}$ |
| 1* | 100 | 77.95 | 0.10 | 0.29 | 0.10 | 0.21 | 499 | 9.0 | 1 | 44.0 | 1 | 57.5 | 1 | 77.9 | 1 | 91.6 |
| 2 | 499 | 8.05 | 0.10 | 0.20 | 0.10 | 0.45 | 421 | 6.8 | 1 | 44.0 | 1 | 57.5 | 1 | 74.8 | 1 | 87.0 |
| 3 | 460 | 8.15 | 0.10 | 0.20 | 0.10 | 0.45 | 424 | 6.4 | 1 | 44.0 | 1 | 57.5 | 1 | 75.0 | 1 | 87.2 |
| **4 (final)** | ***442*** | ***8.25*** | ***0.10*** | ***0.20*** | ***0.10*** | ***0.45*** | ***443*** | ***12.4*** | ***1*** | ***42.0*** | ***1*** | ***54.9*** | ***1*** | ***77.0*** | ***1*** | ***80.7*** |

** remark: uncoordinated design method also gives the same design solution. The units of variables refer to that in Table 1.*

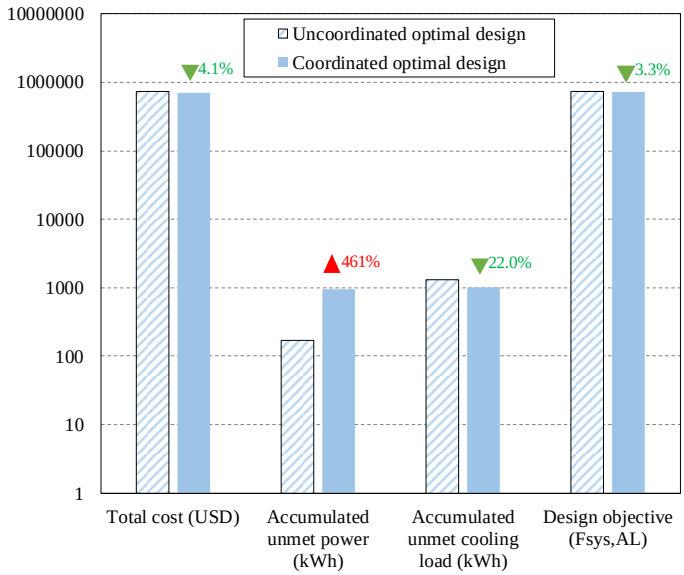


**Fig. 8**. Comparison between energy performance of optimal designs given by coordinated and uncoordinated design methods - standalone low energy building

5.2 Case 2 - Optimal design of a grid-connected low energy building

The optimal design of a grid-connected low energy building is also studied using the coordinated design method and uncoordinated design method respectively. The optimal design solutions are listed in Table 5. Compared with the optimal design solution of the standalone low energy building given by the coordinated design method, smaller capacities of the energy system components are needed for the grid-connected low energy building though their optimal envelope design are similar. This is because it is not economic-efficient to supply electricity using the building-integrated power generation systems than importing electricity from grid when the capacities of energy system components are over certain level.

The optimal design solutions given by uncoordinated design method under different initial PV area settings are also very different for grid-connected low energy building as shown in Table 5. The optimal building envelope design obtained under a smaller PV area setting has much higher building orientation value (closer to east orientation), larger WWR and much smaller overhang projection ratio. The capacities of optimal energy system components are larger except the battery capacity. The results indicate again that uncoordinated design method is not robust to obtain optimal design solutions under different initial settings. The energy performance of the optimal system design solutions given by coordinated design is compared with that given by uncoordinated

design with an initial PV area setting of 100 $m^2$, as shown in Fig. 9. It can be seen that the optimal design given by the coordinated design method has 3.2% ( 21,488 USD) less total cost, 28.8% (533 kWh) less accumulated unmet cooling load ($\Sigma Q_{umt}$) and 3.0% (20,520 USD) less energy system design objective value ($F_{sys,GC}$) compared with the uncoordinated design method, although its accumulated grid impact index ($\Sigma GII$) is 13.2% higher (11). This indicates again that coordinated design method can provide global optimal design solutions, while the design solutions given by uncoordinated design method are "local" optimum.

Table 5. Optimal design solutions of coordinated and uncoordinated design methods - grid-connected low energy building

| Design method | $A_{PV}$ | Optimal envelope design | | | | | Optimal energy system design | | | | | | | | | |
|---|---|---|---|---|---|---|---|---|---|---|---|---|---|---|---|---|
| | | BO | RSA | WWR | WSA | OPR | $A'_{PV}$ | $Cap_{WT}$ | $n_{WT}$ | $Cap_{CG}$ | $n_{CG}$ | $Cap_{AC}$ | $n_{AC}$ | $Cap_{EC}$ | $n_{EC}$ | $Cap_{bat}$ |
| Uncoordinated design | 1032 | 7.55 | 0.1 | 0.2 | 0.10 | 0.44 | 386 | 7.8 | 1 | 30.0 | 1 | 39.0 | 1 | 93.0 | 1 | 77.2 |
| | 100 | 83.75 | 0.1 | 0.29 | 0.1 | 0.20 | 447 | 14.1 | 1 | 30.0 | 1 | 39.2 | 1 | 94.3 | 1 | 57.4 |
| Coordinated design | - | 8.35 | 0.1 | 0.20 | 0.10 | 0.45 | 394 | 25.0 | 0 | 32.0 | 1 | 41.9 | 1 | 89.7 | 1 | 50.1 |

*Note: The units of variables refer to that in Table 1.*

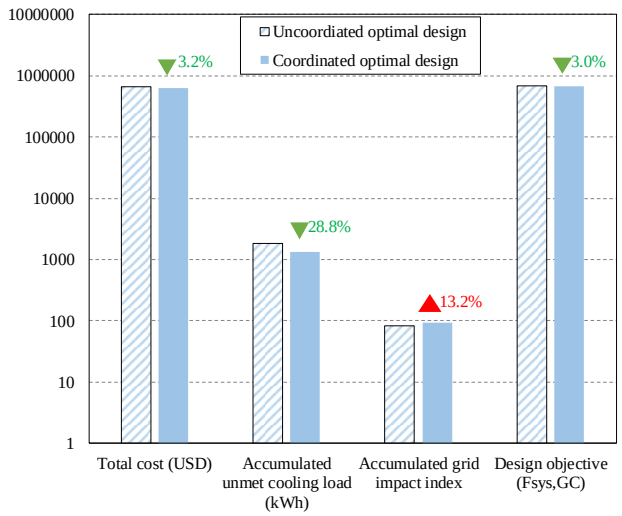


**Fig. 9**. Comparison between energy performance of optimal design solutions given by coordinated and uncoordinated design methods - grid-connected low energy building

5.3 Case 3 - Optimal design of a grid-connected zero energy building

The optimal design of a grid-connected zero energy building is also studied using the coordinated design method and uncoordinated design method respectively. The optimal design solutions are shown in Table 6. The optimal design solutions given by uncoordinated design method under

different initial PV area settings are very different. The optimal building envelope design of grid-connected zero energy building is the same as that of grid-connected low energy building (i.e., Case 2). The optimal energy system design for the optimal envelope design achieved under smaller initial PV area setting has larger capacities for the energy system components except the battery capacity. The results also indicate that uncoordinated design method is not robust to obtain optimal design solutions under different initial settings. The energy performance of optimal system design solutions given by coordinated design is compared with that given by uncoordinated design with the initial PV area setting of 100 $m^2$, as shown in Fig. 10. It can be seen that the optimal design given by coordinated design method has 4.7% (31,796 USD) less total cost, 25.2% (430 kWh) less accumulated unmet cooling load ($\Sigma Q_{umt}$) and 4.6% (31,893 USD) less energy system design objective value ($F_{sys,GC}$) compared with the uncoordinated design method, although its accumulated grid impact index ($\Sigma GII$) is 5.7% higher (5). This indicates again that coordinated design method can provide global optimal design solutions, while the optimal design solutions provided by uncoordinated design method are "local" optimum.

Table 6. Optimal design solutions of coordinated and uncoordinated design methods - grid-connected zero energy building

| Design method | $A_{PV}$ | Optimal envelope design | | | | | Optimal energy system design | | | | | | | | | |
|---|---|---|---|---|---|---|---|---|---|---|---|---|---|---|---|---|
| | | BO | RSA | WWR | WSA | OPR | $A'_{PV}$ | $Cap_{WT}$ | $n_{WT}$ | $Cap_{CG}$ | $n_{CG}$ | $Cap_{AC}$ | $n_{AC}$ | $Cap_{EC}$ | $n_{EC}$ | $Cap_{bat}$ |
| Uncoordinated design | 1032 | 7.55 | 0.1 | 0.2 | 0.10 | 0.44 | 467 | 16.6 | 0 | 30.0 | 1 | 39.2 | 1 | 92.7 | 1 | 61.6 |
| | 100 | 83.75 | 0.1 | 0.29 | 0.1 | 0.20 | 498 | 13.8 | 0 | 32.0 | 1 | 41.8 | 1 | 92.1 | 1 | 54.2 |
| Coordinated design | - | 8.65 | 0.10 | 0.2 | 0.1 | 0.45 | 395 | 8.9 | 0 | 32.0 | 1 | 41.8 | 1 | 89.8 | 1 | 50.4 |

*Note: The units of variables refer to that in Table 1.*

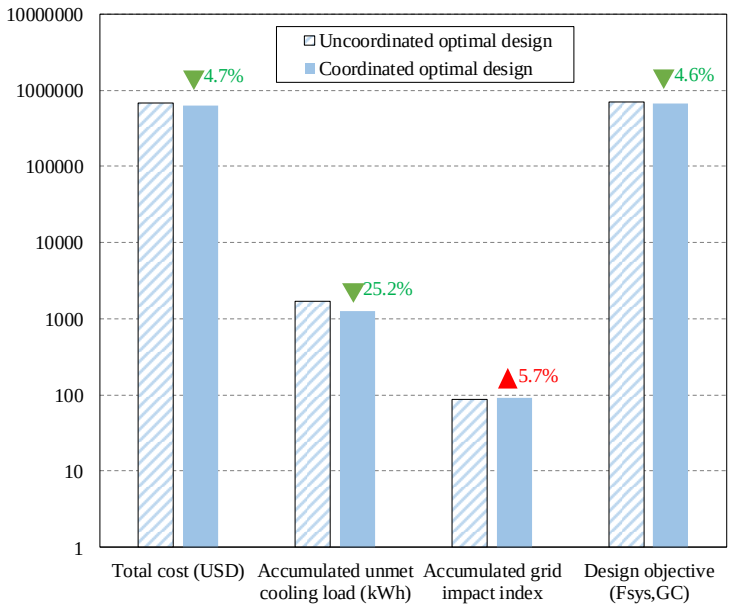


**Fig. 10**. Comparison between energy performance of optimal design solutions given by coordinated and uncoordinated design methods - grid-connected zero energy building

5.4 Discussion on optimization complexity and computation cost

The complexity of optimization and computation cost are other important issues as they are critical especially when a large number of design variables are optimized and simulation software tools are needed to assess the building performance and energy system performance. To achieve the global optimal design solution of a building, the design optimizations of its building envelope and energy systems need to be considered as a whole, which is typically achieved by simultaneous optimization methods. For example, when simultaneous optimization methods are used for the validation case, EnergyPlus or other building simulation software is needed for building performance evaluation. This is because hourly data are required for the energy system performance evaluation while the ANN model cannot provide hourly performance data. The computation time for the GA-based simultaneous optimization of the building envelope and energy systems, using EnergyPlus (instead of ANN building model), is estimated to be about 119 hours if assuming the same evaluation times (i.e. 20,000 times = 100 generations x 200 populations, for the energy system optimization in the above case studies) are needed. This estimated minimum computation time is 5 times of that using the coordinated design method (23.5 hours on a regular PC). The actual computation time could be much longer as it would actually need much more evaluation times as 15 design variables (instead of 10 design variables for system design

optimization) are involved. In such case and other cases involving more design variables, the computation time of simultaneous optimization method would be impractically long and unaffordable. Compared with the existing simultaneous design optimization methods, the coordinated design method proposed in this study can achieve the global optimal design solution approximately with significantly reduced computation cost and optimization complexity.

## 6. Conclusions

Based on the results and experiences from the case studies, conclusions can be made as follows. The optimizations of building envelope design and energy system design need to be integrated as a coordinated design process when some system design variables optimized at later stage have impacts on building envelope design optimization ( earlier stage).

The proposed method is robust in providing optimal design solutions for zero/low energy buildings and their energy systems. The case studies show that coordinated optimal design can always converge to the same optimal design solution under different initial settings although different iteration times may be needed, while design solutions of uncoordinated design method could be very different under different initial settings.

The proposed method can provide "global" optimal design solutions for zero/low energy buildings and their energy systems, while the optimal design solutions given by the uncoordinated multi-stage design optimization method could be "local" optimum. For the validation case, the total cost and design objective value of the optimal energy systems given by the coordinated design method are about 4% less compared with the uncoordinated design method, and their accumulated unmet cooling loads decrease by over 22%.

The proposed method can efficiently achieve the global optimal design solution that needs to consider building envelope and building energy systems as a whole in the optimization. This is typically achieved by simultaneous design optimization method while the proposed method could achieve similar effect with much reduced optimization complexity and computation cost. The experience of the case studies shows that the actual computation cost is about 3 or 4 times of that of multi-stage design optimization method but is much less than simultaneous optimization methods, which might need impractically long and unaffordable computation time. The proposed method has essential advantage particularly when the numbers of design variables are large.

**Acknowledgement**

The research presented in this paper is financially supported by a grant (152079/18E) of the Research Grant Council (RGC) of the Hong Kong SAR.

**Reference**

1. Manila-Paris Declaration of the Climate Vulnerable Forum.
2. Environment Bureau. Hong Kong climate action plan 2030+, 2017. Available at: https://www.enb.gov.hk/sites/default/files/pdf/ClimateActionPlanEng.pdf
3. International Energy Agency. Key world energy statistics, 2017.
4. EMSD. Hong Kong Energy End-use Data, 2016. Available at: http://www.emsd.gov.hk/emsd/eng/pee/edata_1.shtml.
5. Mohamed A, Hasan A, Sirén K. Fulfillment of net-zero energy building (NZEB) with four metrics in a single family house with different heating alternatives. Applied Energy 2014; 114: 385-399.
6. Leckner M, Zmeureanu R. Life cycle cost and energy analysis of a Net Zero Energy House with solar combisystem. Applied Energy 2011; 88: 232-241.
7. Li HX, Wang SW, Cheung H. Sensitivity analysis of design parameters and optimal design for zero/low energy buildings in subtropical regions. Applied Energy 2018; 228: 1280-1291.
8. Thalfeldt M, Pikas E, Kurnitski J, Voll H. Façade design principles for nearly zero energy buildings in a cold climate. Energy and Buildings 2013; 67: 309-321.
9. Lu YH, Wang SW, Zhao Y, Yang CC. Renewable energy system optimization of low/zero energy buildings using single-objective and multi-objective optimization methods. Energy and Buildings 2015; 89: 61-75.
10. Kaabeche A, Ibtiouen R. Techno-economic optimization of hybrid photovoltaic/wind/diesel/battery generation in a stand-alone power system. Solar Energy 2014; 103: 171-182.
11. Ismail MS, Moghavvemi M, Mahlia TMI. Design of a PV/diesel stand alone hybrid system for a remote community in Palestine. Journal of Asian Scientific Research 2012; 2(11): 599-606.

12. Lu YH, Wang SW, Shan K. Design optimization and optimal control of grid-connected and standalone nearly/net zero energy buildings. Applied Energy 2015; 155: 463-477.

13. Lu YH, Wang SW, Yan CC, Shan K. Impacts of renewable energy system design inputs on the performance robustness of net zero energy buildings. Energy 2015; 93: 1595-1606.

14. Daud AK, Ismail MS. Design of isolated hybrid systems minimizing costs and pollutant emissions. Renewable Energy 2012; 44: 215-224.

15. José LBA, Rodolfo DL. Simulation and optimization of standalone hybrid renewable energy systems. Renewable and Sustainable Energy Reviews 2009; 13(8): 2111-2118.

16. Diaf S, Belhamel M, Haddadi M, Louche A. Technical and economic assessment of hybrid photovoltaic/wind system with battery storage in Corsica island. Energy Policy 2008; 36(2): 743-754.

17. Zhang S, Huang P, Sun YJ. A multi-criterion renewable energy system design optimization for net zero energy buildings under uncertainties. Energy 2016; 94: 654-665.

18. Marszal AJ, Heiselberg P. Life cycle cost analysis of a multi-storey residential Net Zero Energy Building in Denmark. Energy 2011; 36: 5600-5609.

19. Georges L, Massart C, Moeseke GV, Herde AD. Environmental and economic performance of heating systems for energy-efficient dwellings: Case of passive and low-energy single-family houses. Energy Policy 2012; 40: 452-464.

20. Ferrara M, Fabrizio E, Virgone J, Filippi M. A simulation-based optimization method for cost-optimal analysis of nearly Zero Energy Buildings. Energy ad Buildings 2014; 84: 442-457.

21. Hamdy M, Palonen M, Hasan Ala. Implementation of pareto-archive NSGA-II algorithms to a nearly-zero-energy building optimisation problem. First Building Simulation and Optimization Conference. Loughborough, UK, 10-11 September, 2012.

22. Kapsalaki M, Leal V, Santamouris M. A methodology for economic efficient design of Net Zero Energy Buildings. Energy and Buildings 2012; 55: 765-778.

23. Hamdy M, Hasan A, Siren K. A multi-stage optimization method for cost-optimal and nearly-zero-energy building solutions in line with the EPBD-recast 2010. Energy and Buildings 2013; 56: 189-203.

24. Kurnitski J, Saari A, Kalamees T, Vuolle M, Niemelä J, Tark T. Cost optimal and nearly zero (nZEB) energy performance calculations for residential buildings with REHVA definition for nZEB national implementation. Energy and Buildings 2011; 43: 3279-3288.

25. Rysanek AM, Choudhary R. A decoupled whole-building simulation engine for rapid exhaustive search of low-carbon and low-energy building refurbishment options. Building and Environment 2012; 50: 21-33.

26. D'Agostino D, Parker D. A framework for the cost-optimal design of nearly zero energy buildings (NZEBs) in representative climates across Europe. Energy 2018; 149: 814-829.

27. Ascione F, Bianco N, De Stasio, C., Mauro, G. M., & Vanoli, G. P. (2016). Multi-stage and multi-objective optimization for energy retrofitting a developed hospital reference building: A new approach to assess cost-optimality. Applied energy, 174, 37-68.

28. Ascione, F., Bianco, N., De Masi, R. F., Mauro, G. M., & Vanoli, G. P. (2017). Resilience of robust cost-optimal energy retrofit of buildings to global warming: A multi-stage, multi-objective approach. Energy and Buildings, 153, 150-167.

29. Ascione, F., Bianco, N., Mauro, G. M., & Vanoli, G. P. (2019). A new comprehensive framework for the multi-objective optimization of building energy design: Harlequin. Applied energy, 241, 331-361.

30. Ting CK. On the mean convergence time of multi-parent genetic algorithms without selection. European Conference on Artificial Life 2005: 403-412.

31. Construction Industry Council. Zero Carbon Design. Available at: https://zcb.cic.hk/eng/home

32. Chen X, Yang HX, Zhang WL. Simulation-based approach to optimize passively designed buildings: A case study on a typical architectural form in hot and humid climates. Renewable and Sustainable Energy Reviews 2018; 82: 1712-1725.

33. Fanger PO. Thermal comfort: Analysis and applications in environmental engineering. McGraw-Hill; 1972.

34. Maheri A. Multi-objective design optimisation of standalone hybrid wind-PV-diesel systems under uncertainties. Renewable Energy 2014; 66: 650-661.

35. Liu MX, Shi Y, Fang F. A new operation strategy for CCHP systems with hybrid chillers. Applied Energy 2012; 95: 164-173.

36. Gang WJ, Wang SW, Xiao F, Gao DC. Robust optimal design of building cooling systems considering cooling load uncertainty and equipment reliability. Applied Energy 2015; 159: 265-275.

37. Nottrott A, Kleissl J, Washom B. Energy dispatch schedule optimization and cost benefit analysis for grid-connected, photovoltaic-battery storage systems. Renewable Energy 2013; 55: 230-240.

38. Huang P, Huang GS, Sun YJ. A robust design of nearly zero energy building systems considering performance degradation and maintenance. Energy 2018; 163: 905-919.

39. Helton JC, Davis FJ. Latin hypercube sampling and the propagation of uncertainty in analyses of complex systems. Reliability Engineering & System Safety 2003; 81(1): 23-69.

40. Kohavi R. A study of cross-validation and bootstrap for accuracy estimation and model selection. International Joint Conference on Artificial Intelligence 1995.

41. Linssen J, Stenzel P, Fleer J. Techno-economic analysis of photovoltaic battery systems and the influence of different consumer load profiles. Applied Energy 2017; 185: 2019-2025.